

RESEARCH

Open Access



# Identification of novel sublingual parameters to analyze and diagnose microvascular dysfunction in sepsis: the NOSTRADAMUS study

Alexandros Rovas<sup>1</sup>, Jan Sackarnd<sup>2</sup>, Jan Rossaint<sup>3</sup>, Stefanie Kampmeier<sup>4</sup>, Hermann Pavenstädt<sup>1</sup>, Hans Vink<sup>5†</sup> and Philipp Kümpers<sup>1\*†</sup> 

## Abstract

**Background:** The availability of handheld, noninvasive sublingual video-microscopes allows for visualization of the microcirculation in critically ill patients. Recent studies demonstrate that reduced numbers of blood-perfused microvessels and increased penetration of erythrocytes into the endothelial glycocalyx are essential components of microvascular dysfunction. The aim of this study was to identify novel microvascular variables to determine the level of microvascular dysfunction in sepsis and its relationship with clinical variables.

**Methods:** This observational, prospective, cross-sectional study included 51 participants, of which 34 critically ill sepsis patients were recruited from intensive care units of a university hospital. Seventeen healthy volunteers served as controls. All participants underwent sublingual videomicroscopy by sidestream darkfield imaging. A new developed version of the Glycocheck™ software was used to quantify vascular density, perfused boundary region (PBR—an inverse variable of endothelial glycocalyx dimensions), red blood cell (RBC) velocity, RBC content, and blood flow in sublingual microvessels with diameters between 4 and 25 μm.

**Results:** A detailed analysis of adjacent diameter classes (1 μm each) of vessels between 4 and 25 μm revealed a severe reduction of vascular density in very small capillaries (5–7 μm), which correlated with markers of sepsis severity. Analysis of RBC velocity ( $V_{RBC}$ ) revealed a strong dependency between capillary and feed vessel  $V_{RBC}$  in sepsis patients ( $R^2 = 0.63$ ,  $p < 0.0001$ ) but not in healthy controls ( $R^2 = 0.04$ ,  $p = 0.43$ ), indicating impaired capillary (de-)recruitment in sepsis. This finding enabled the calculation of capillary recruitment and dynamic capillary blood volume ( $CBV_{dynamic}$ ). Moreover, adjustment of PBR to feed vessel  $V_{RBC}$  further improved discrimination between sepsis patients and controls by about 50%. By combining these dynamic microvascular and glycocalyx variables, we developed the microvascular health score ( $MVHS_{dynamic}^{TM}$ ), which decreased from 7.4 [4.6–8.7] in controls to 1.8 [1.4–2.7] in sepsis patients ( $p < 0.0001$ ) and correlated with sepsis severity.

**Conclusion:** We introduce new important diameter-specific quantification and differentiated analysis of RBC kinetics, a key to understand microvascular dysfunction in sepsis.  $MVHS_{dynamic}$ , which has a broad bandwidth to detect microvascular (dys-) function, might serve as a valuable tool to detect microvascular impairment in critically ill patients.

\*Correspondence: philipp.kuempers@ukmuenster.de

†Hans Vink and Philipp Kümpers have contributed equally and are both considered senior authors

<sup>1</sup> Department of Medicine D, Division of General Internal and Emergency Medicine, Nephrology, and Rheumatology, University Hospital Münster, Albert-Schweitzer-Campus 1, 48149 Münster, Germany  
Full list of author information is available at the end of the article



**Keywords:** Endothelial glycocalyx, Capillary recruitment, Perfused boundary region, Microvascular health score, Sepsis

## Background

Alterations of microvascular perfusion caused by endothelial cell dysfunction, glycocalyx degradation, increased leukocyte adhesion, microthrombus formation, and regional redistribution of blood flow contribute to organ failure in critically ill patients [1–3]. The use of handheld, noninvasive sublingual video microscopes, such as incident dark field (IDF) or sidestream dark field (SDF) microscopy, allows researchers to visualize and analyze microvascular perfusion alterations in vivo [4, 5]. Over the past decade, several measures of microvascular perfusion variables have been proposed to improve risk stratification, prognostication and eventually to individualize the therapy, especially in critically ill patients with sepsis and septic shock [6–13]. Despite tremendous efforts to improve video quality and standardize reporting, the quantitative analysis of functional measures remains challenging and is often performed manually [6]. Several visual scoring systems and specialized (semi-) automated analysis tools have been developed to shorten time-to-result and improve accuracy [14–17]. Common to all these approaches is the (automated) selection and pooled analysis of microvessels with a diameter < 20 (rarely < 10)  $\mu\text{m}$ . An improved spatiotemporal resolution within this < 20  $\mu\text{m}$  range is desirable to further dissect and understand functional microvascular alterations in sepsis and critical illness.

We have previously used the Glycocheck™ System to analyze the perfused boundary region (PBR), an inverse variable of endothelial glycocalyx (eGC) dimensions, in sublingual microvessels from sepsis patients [18–20]. The software automatically detects, records, and analyzes the PBR according to diameter classes (each 1  $\mu\text{m}$ ) in microvessels with diameters between 4 and 25  $\mu\text{m}$ . The methodology showed very good inter- and intra-observer reproducibility under real-life conditions [19] and excellent accuracy compared to other in vitro and ex vivo estimations of eGC thickness [18, 20, 21]. The aim of this study was to identify novel dynamic microvascular variables generated by a new diameter-class-wise approach to determine the level of microvascular dysfunction in sepsis and its relationship with established clinical variables and the number of dysfunctional organs.

## Materials and methods

### Study population

This prospective, observational, cross-sectional study took place in the medical and operative ICUs of the

University Hospital Münster. The study was performed in accordance with the Declaration of Helsinki and was approved by the competent ethics committee (amendment to 2016-073-f-S). Some of the participants were already included in previous studies on eGC damage in sepsis [18, 20].

After written informed consent was obtained from the patients or their legal representatives, 34 adult ICU patients with sepsis were enrolled non-consecutively after initial resuscitation. Sepsis was defined by the sepsis-3 criteria published by the ESICM-SCCM Sepsis Redefinitions Task Force [22]. Exclusion criteria were age < 18 years, pregnancy, or oral mucosal inflammation or injury, which could locally influence the sublingual microvasculature. Seventeen apparently healthy volunteers served as controls.

Demographic variables, routine chemistry tests, and physiological variables, including the Sequential Organ Failure Assessment (SOFA) score [22] and a contemporary version of the Charlson Comorbidity Index (CCI) [23], were obtained for each subject at the time of sublingual videomicroscopy (Table 1). Each videomicroscopy set consisted of two complete measurements (see below) which were averaged to account for spatial heterogeneity of the sublingual microvasculature.

### Video acquisition and analysis of the sublingual microvasculature

Figure 1 provides an overview of the process of video acquisition, data analysis and post-processing. Bedside intravital microscopy was performed with a sidestream dark field (SDF) camera (CapiScope HVCS, KK Technology, Honiton, UK) to visualize the sublingual microvasculature according to a standardized procedure as described in detail previously [20]. A physician experienced in the SDF technique, trained to recognize and avoid pressure artifacts performed the image acquisition based on the current round table recommendations [6]. The SDF camera uses green light-emitting stroboscopic diodes (540 nm) to detect the hemoglobin of passing red blood cells (RBCs). Using a 5 $\times$  objective with a 0.2 numerical aperture, images were captured, providing a 325-fold magnification in 720 $\times$ 576 pixels at 23 frames per second as described in detail previously [19, 24, 25].

The analysis of all variables was carried out exclusively with the GlycoCheck™ Software (Microvascular Health Solutions Inc., Salt Lake City, UT, USA) software. Briefly, the GlycoCheck™ Software allows video

**Table 1** Baseline characteristics

Variable	Healthy controls	Sepsis patients	<i>p</i> value
Number of participants ( <i>n</i> ; %)	17	34	–
Female sex ( <i>n</i> ; %)	9 (53)	8 (24)	0.06
Age (years, median (IQR))	51 (33–72)	66 (56–78)	0.06
BMI (kg/m <sup>2</sup> , median (IQR))	23 (21.5–24.9)	25.8 (21.9–29.2)	0.06
Duration of sepsis at study inclusion (days, median (IQR))*	–	2 (1–4)	–
SOFA score (median (IQR))	–	10 (8–13)	–
Number of dysfunctional organs (median (IQR))	–	4 (3–5)	–
Organ replacement therapy ( <i>n</i> ; %)	–	22 (64.7)	–
Mechanical ventilation ( <i>n</i> ; %)	–	21 (61.8)	–
Acute dialysis ( <i>n</i> ; %)	–	6 (17.7)	–
Vasopressors ( <i>n</i> ; %)	–	26 (76.4)	–
Norepinephrine dose (µg/kg/min)	–	0.06 (0.02–0.14)	–
Septic shock ( <i>n</i> ; %)*	–	6 (17.7)	–
Inhospital mortality ( <i>n</i> ; %)	–	13 (38.2)	–
CCI score (median (IQR))	–	2 (1–3)	–
<i>Macrocirculation data</i> (median (IQR))			
MAP (mmHg)	95.3 (86–98.7)	71.8 (66.5–81.1)	<0.0001
Heart Rate (pulse/min)	72 (65–83)	90 (75–102)	0.0002
Respiratory Rate (breaths/min)	14 (12–15)	21 (18–26)	<0.0001
Temperature (°C)	36.6 (36.5–36.9)	36.9 (36.4–37.7)	0.08
<i>Laboratory data</i> (median (IQR))			
CRP (mg/dl)	0.5	22.4 (16.9–33.3)	<0.0001
IL-6 (ng/ml)	2 (2–3)	452 (137–1121)	<0.0001
PCT (ng/ml)	0.05 (0.04–0.07)	17.43 (2.04–52.44)	<0.0001
pH	–	7.41 (7.35–7.45)	–
Lactate (mmol/l)	1.1 (0.80–1.4)	1.70 (1.08–2)	0.004

*BMI* Body mass index, *CCI score* Charlson Comorbidity Index, *CRP* C-reactive protein, *IL-6* Interleukin-6, *IQR* interquartile range, *MAP* Mean arterial pressure, *PCT* Procalcitonin, *SOFA score* Sequential Organ Failure Assessment score

\*Septic shock: Vasopressors required to maintain MAP ≥ 65 mmHg AND serum lactate > 2 mmol/l. *p* value was calculated between healthy controls and sepsis patients

acquisition after predefined image quality criteria (motion, intensity, and focus) are fulfilled. Specifically, light intensity range is automatically set to prevent under- or over-exposure of the video. The acceptable motion range is set so that every vessel can be tracked in all frames of each video. Each complete measurement consists of at least ten 2-s videos (40 frames/video), containing a total of about 3000 vascular segments of 10 µm length each. All videos are deliberately obtained from different positions to counterbalance spatial heterogeneity of the sublingual microcirculation. The software automatically subjects the obtained vascular segments to a strict quality check, as previously described in detail [25]. Briefly, vascular segments are considered valid only if: (1) red blood cell content is ≥ 50%, (2) RBC width is ≥ 2 µm, (3) segments are neither curved, (4) nor too close to each other. Invalid vascular segments are marked yellow and are automatically discarded, while all valid vascular segments (green lines) are further analyzed. Therefore, all

further parameters are calculated based on these valid segments. Screenshots of the sublingual mucosa of five randomly chosen individuals are shown in Additional file 1: Fig. S1 (with and without automatically acquired vessel detection and quality check). Moreover, two additional movie files illustrate the sublingual mucosa of a healthy control and a sepsis individual with and without automatic vessel detection and subsequent quality check in more detail (Additional file 2: Video 1, Additional file 3: Video 2). Finally, the software obtains up to 840 radial intensity profiles for each valid vascular segment based on the RBC column width (RBCW), and automatically groups vessels from 4 to 25 µm diameter in 22 separate diameter classes (1 µm each). This concept has been successfully used and validated in the past [25]. Data from two complete measurements (hereafter referred to as “measurement set”) were extracted, analyzed, and averaged offline to avoid sampling error and to counterbalance spatiotemporal heterogeneity of the sublingual microcirculation [19, 20].

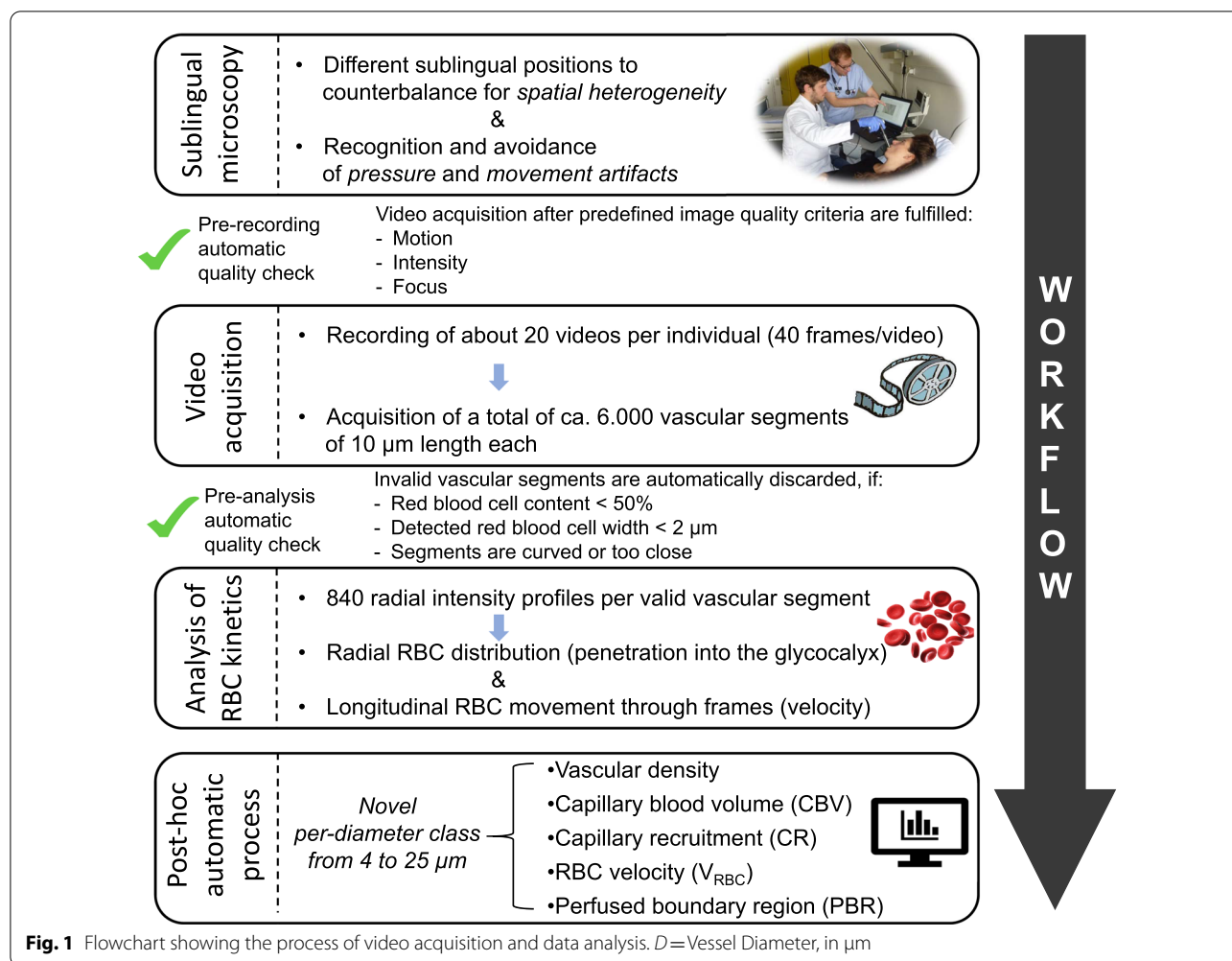


**Fig. 1** Flowchart showing the process of video acquisition and data analysis.  $D$ =Vessel Diameter, in  $\mu\text{m}$

### RBC velocity

Valid red blood cell (RBC) velocities ( $V_{\text{RBC}}$ ) are determined in individual vessel segments in an automatic fashion by cross correlation of longitudinal RBC intensity profiles between frames of recorded videos. A correlation coefficient of  $\geq 0.80$  was required to ensure accurate estimates of longitudinal RBC displacement. RBC velocity is determined by dividing RBC displacement by the time between video frames and expressed as  $\mu\text{m/s}$ . The automatic estimation of the  $V_{\text{RBC}}$  correlated excellently with a manual analysis ( $R^2 = 0.94$ ,  $p < 0.0001$ ; Additional file 4: Fig. S2).

### Perfused vascular and capillary density

An absolute measure for valid perfused vascular density ( $\text{mm/mm}^2$ ) can be determined from the number of vascular segments containing RBCs multiplied by capillary segment length (each 10  $\mu\text{m}$ ). All detected RBC-containing vessel segments (RBC content  $\geq 50\%$ ) with

$V_{\text{RBC}} \geq 0 \mu\text{m/s}$  were automatically counted in the video recordings of each subject. Vascular density was normalized to tissue surface area. As *non-perfused* vessels (i.e., without RBCs present), as well as vessels not meeting the quality criteria cannot be detected by our methodology, therefore vascular density in this manuscript refers to *valid perfused* vascular density (hereafter vascular density). *Capillary* density was defined as vascular density of vessels with a diameter equal or smaller than the diameter of a single red blood cell (RBC diameter  $\sim 7$  to  $8 \mu\text{m}$  [26]; capillary density  $D \leq 7 \mu\text{m}$ ).

### Absolute and static capillary blood volume

An absolute measure for valid capillary blood volume ( $\text{CBV}_{\text{absolute}}$ ) can be determined from the number of capillary segments multiplied by capillary segment length (i.e., capillary density ( $\text{mm/mm}^2$ )) and segment-specific capillary cross-sectional area ( $\pi * \text{radius}^2$ ). In addition to counting the number of RBC-containing

capillary segments, a functional estimate of CBV relative to larger vessel blood volume can be determined by measuring average  $V_{RBC}$  in capillaries and larger blood vessels (hereafter feed vessels). The corresponding  $V_{RBC}$  ratio in feed vessels (diameter 10 to 25  $\mu\text{m}$ , hereafter  $D \geq 10 \mu\text{m}$ ) over  $V_{RBC}$  in capillaries (diameter 4 to 7  $\mu\text{m}$ , hereafter  $D \leq 7 \mu\text{m}$ ) denotes the CBV ratio ( $= V_{RBC}(D \geq 10 \mu\text{m}) / V_{RBC}(D \leq 7 \mu\text{m})$ ). In short, an increase in capillary blood volume relative to feed vessel blood volume will reduce capillary  $V_{RBC}$  and this will increase the CBV ratio. Multiplying the  $CBV_{\text{absolute}}$  with the CBV ratio gives the static capillary blood volume ( $CBV_{\text{static}}$ ), which is defined as:  $CBV_{\text{static}} = CBV_{\text{absolute}} * V_{RBC}(D \geq 10 \mu\text{m}) / V_{RBC}(D \leq 7 \mu\text{m})$ .

**Capillary recruitment and dynamic capillary blood volume**

To take the ability to recruit additional capillaries into account, an estimate can be made of the capillary recruitment (CR) by measuring the slope of the relationship between  $V_{RBC}(D \leq 7 \mu\text{m})$  and  $V_{RBC}(D \geq 10 \mu\text{m})$ . When the number of blood perfused capillaries increases upon and increase in  $V_{RBC}(D \geq 10 \mu\text{m})$ , the accompanying increase in  $V_{RBC}(D \leq 7 \mu\text{m})$  will be less than proportional (i.e., the regression slope will be  $< 1$ ) and capillary recruitment can be defined as  $1 - \text{slope}(V_{RBC}(D \leq 7 \mu\text{m}), V_{RBC}(D \geq 10 \mu\text{m}))$ . Two extreme examples of this concept are shown in Additional file 5: Fig. S3: In case capillary blood volume doubles when large vessel RBC velocity increases twofold, the slope( $V_{RBC}(D \leq 7 \mu\text{m}), V_{RBC}(D \geq 10 \mu\text{m})$ ) will be 0 and  $CR = 1 - \text{slope } 0 = 1 = 100\%$ . In the absence of changes in capillary blood volume when  $V_{RBC}(D \geq 10 \mu\text{m})$  increases twofold, capillary RBC velocities are expected to also change proportionally by twofold, and the slope of  $V_{RBC}(D \leq 7 \mu\text{m})$  vs.  $V_{RBC}(D \geq 10 \mu\text{m})$  will be 1 and  $CR = 1 - \text{slope } 1 = 0 = 0\%$ . Multiplying the  $CBV_{\text{static}} * (1 + CR)$  gives the dynamic capillary blood volume ( $CBV_{\text{dynamic}}$ ).

**Static and dynamic perfused boundary region (PBR)**

The software calculates the dynamic lateral movement of RBCs into the permeable part of the eGC layer, expressed as the PBR (in  $\mu\text{m}$ ). An impaired eGC permits a greater number of RBCs to penetrate deep into the endothelium, which is translated as an increase in the PBR value. The radial distribution of RBCs in each valid segment defines the median RBC width (RBCW), as well as the outer edge of the RBC-perfused vessel diameter ( $D_{\text{perf}}$ ). The  $PBR_{\text{static}}$  is defined as the distance between the RBCW and  $D_{\text{perf}}$  and is calculated using the following formula:  $(D_{\text{perf}} - RBCW) / 2$  [25].

In line with the above-described measures of velocity-dependent increases in capillary blood volume, it

is possible that also penetration of RBCs into the luminal glycocalyx surface (as reflected by PBR) is velocity-dependent. To minimize possible flow-dependent variability in PBR estimation, the slope( $PBR_{\text{static}}, V_{RBC}(D \geq 10 \mu\text{m})$ ) can be used to  $PBR_{\text{dynamic}}$  under equal conditions, i.e., the absence of RBC velocity ( $V_{RBC}(D \geq 10 \mu\text{m})$  set to 0  $\mu\text{m/s}$ ) (Additional file 6: Fig. S4 for details).

**Statistical analysis**

Data are presented as absolute numbers, percentages, or medians with corresponding 25th and 75th percentiles (interquartile range; IQR), as appropriate. The nonparametric Mann–Whitney U test and the chi-square test were used to compare variables between patients and controls. To correct for multiple testing in comparisons of microcirculation variables per-diameter class we used the false discovery rate (FDR) approach of Benjamini, Krieger and Yekutieli, setting a  $q$ value  $< 0.05$  as significant. Spearman rank correlation coefficient was used to assess correlations between clinical and microvascular variables. Associations between microvascular measures were evaluated using simple and adjusted linear regression models. All the tests used were two-sided, and statistical significance was set at  $p < 0.05$ . Our study was powered to detect a moderate correlation (Spearman correlation coefficient = 0.5) between microvascular health score and SOFA score in the septic cohort with 85% power given a two-sided alpha of 0.05 [27]. SPSS version 26 (IBM Corporation, Armonk, NY, USA) and GraphPad Prism version 8.4.3 (GraphPad Prism Software Inc., San Diego, CA, USA) were used for statistical analyses and preparation of figures.

**Results**

The clinical and demographic characteristics of the 51 study participants are shown in Table 1 and Additional file 7: Table A1. 50% of the patients had a respiratory focus of infection, while the remainder demonstrated other etiologies (Additional file 7: Table A1). From a total of 34 sepsis patients, 22 (65%) required organ replacement therapy (mechanical ventilation or/and renal replacement therapy) and 26 (76%) were vasopressor-dependent at study inclusion. Our sepsis cohort had a median (IQR) SOFA score of 10 (8–13), indicating moderate disease severity. The median time of sepsis begin was 2 days (1–4) and 6 (18%) patients had septic shock (Sepsis-3 definitions: lactate  $> 2$  mmol/l and need for vasopressors to maintain a mean arterial pressure  $\geq 65$  mm Hg) at the time of study inclusion.



### Analysis of sublingual microcirculation according to vessel diameter class

First, we compared vascular density,  $V_{RBC}$  and  $PBR_{static}$  between healthy controls and sepsis patients in a diameter-class-wise fashion. This approach revealed a statistically significant decrease in vascular density only in the diameter classes 5, 6 and 7  $\mu\text{m}$  in sepsis patients ( $-63\%$ ,  $-42\%$ , and  $-28\%$  compared to controls), whereas the

remaining diameter classes from 8 to 25  $\mu\text{m}$  were not different between the groups (Fig. 2a and Additional file 8: Fig. S5). However, vascular density was not different between the groups in a pooled analysis (4–25  $\mu\text{m}$  range) ( $12.3$  vs.  $12.8$   $\text{mm}/\text{mm}^2$ ,  $p=0.34$ ). To check our results for plausibility, we correlated, in an explorative manner, vascular density with clinical variables, such as interleukin-6 (IL-6), procalcitonin (PCT), lactate and

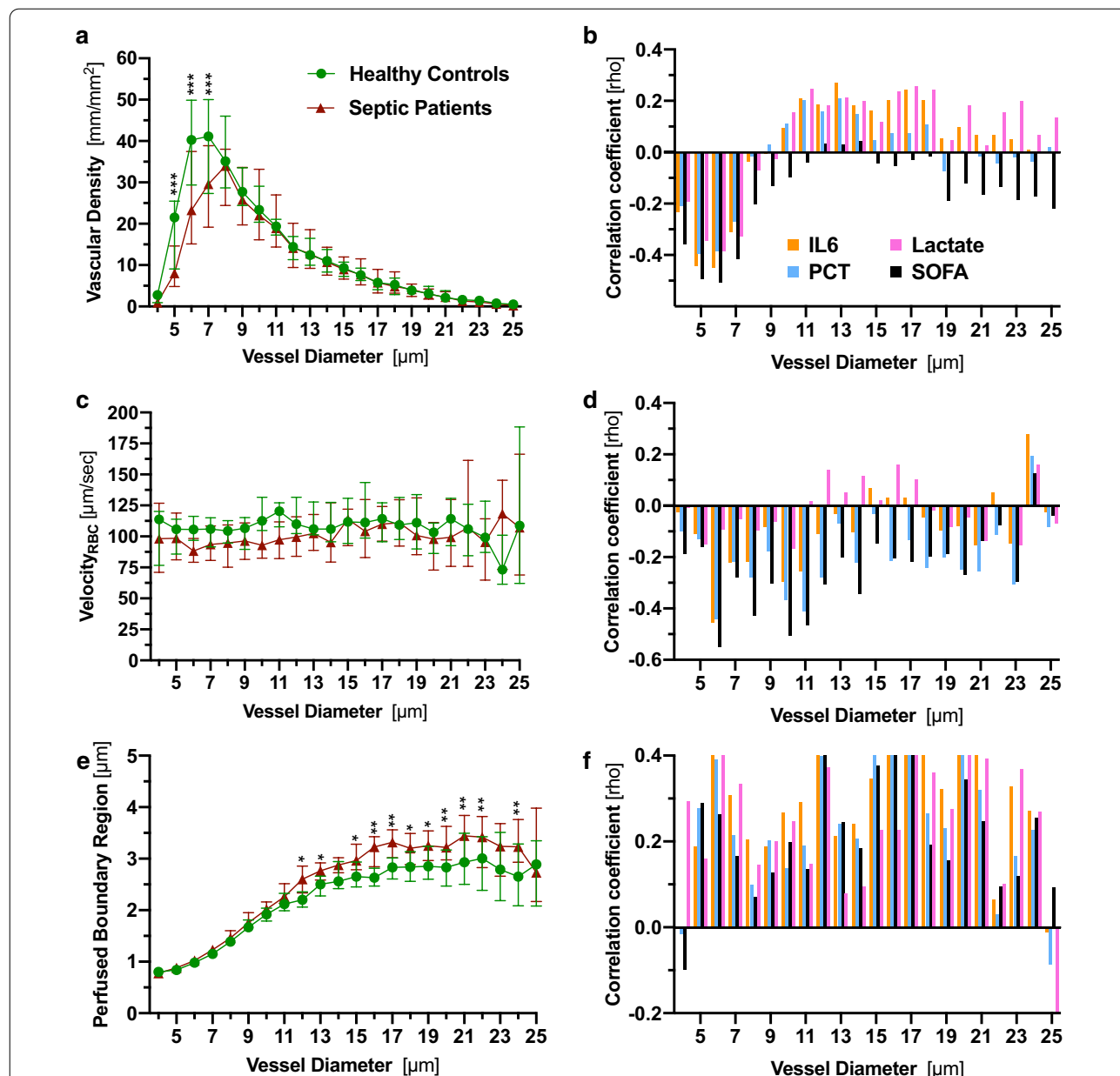


**Fig. 2** Analysis of sublingual microcirculation according to vessel diameter class. **a, c, e** Median and IQR values of vascular density,  $PBR_{static}$  values and RBC velocity of healthy controls and sepsis patients according to diameter class from 4 to 25  $\mu\text{m}$ . **b, d, f** Bar charts showing the correlation coefficient (Spearman) between microvascular and clinical variables. IQR inter quartile range, IL6 interleukin 6,  $PBR$  perfused boundary region, PCT procalcitonin, RBC red blood cell, SOFA score sequential organ failure assessment score. Q value (adjusted p value): \* $q < 0.05$ , \*\* $q < 0.01$ , \*\*\* $q < 0.001$

SOFA score. We found a robust inverse correlation in the 4 to 7  $\mu\text{m}$  diameter range, while these associations were absent or even partially reversed in larger vessels (Fig. 2b and Additional file 7: Table A2).

$V_{\text{RBC}}$  showed a huge overlap between patients and controls. Median  $V_{\text{RBC}}$  trended to be slightly lower in sepsis patients, especially in smaller vessels and was inversely correlated with variables of disease severity (Fig. 2c, d and Additional file 7: Table A2). A significant sepsis-induced increase in  $\text{PBR}_{\text{static}}$  was particularly apparent in feed vessels, probably due to loss of the affected smaller vessels (lower capillary density) (Fig. 2e and Additional file 9: Fig. S6).  $\text{PBR}_{\text{static}}$  values of individual diameter classes showed weak-to-moderate positive correlations with variables of sepsis severity (Fig. 2f and Additional file 7: Table A2).

Taken together, the diameter class-wise data analysis revealed individual sepsis-induced perturbations in vascular density,  $V_{\text{RBC}}$  and  $\text{PBR}_{\text{static}}$ .

#### Derivation of capillary recruitment and dynamic capillary blood volume.

Having observed a significant decrease in vascular density in very small capillaries (diameter ( $D$ )  $\leq 7 \mu\text{m}$ ) in sepsis patients, we determined and focused on the capillary blood volume (Fig. 3).  $\text{CBV}_{\text{absolute}}$  decreased from 16.5 [10.3–19.4]  $10^3 \mu\text{m}^3$  in healthy controls to 7.9 [5.9–14.5]  $10^3 \mu\text{m}^3$  in sepsis patients ( $p = 0.006$ ). To further improve discrimination between the groups, we added some functional variables to the CBV calculation.

First, we calculated  $\text{CBV}_{\text{static}}$  by multiplying  $\text{CBV}_{\text{absolute}}$  with a ratio derived from  $V_{\text{RBC}}$  in feed vessels relative to capillaries ( $V_{\text{RBC}} (D \geq 10 \mu\text{m}) / V_{\text{RBC}} (D \leq 7 \mu\text{m})$ ). However, the suspected decrease in the CBV ratio (due to decrease in capillary density) in sepsis patients did not occur (Fig. 3a). The reason for this only became apparent after plotting capillary  $V_{\text{RBC}} (D \leq 7 \mu\text{m})$  as a function of large vessel  $V_{\text{RBC}} (D \geq 10 \mu\text{m})$  (Fig. 3b). This type of analysis revealed a strong dependency between  $V_{\text{RBC}} (D \leq 7 \mu\text{m})$  and  $V_{\text{RBC}} (D \geq 10 \mu\text{m})$  in sepsis patients ( $R^2 = 0.63$ ,  $p < 0.0001$ ), indicating impaired capillary (de-)recruitment in this group. In contrast, capillary  $V_{\text{RBC}}$  is relatively constant in healthy controls as reported before [28], indicating functioning (de-)recruitment of CBV associated with changes of feed vessel blood flow in healthy subjects.  $\text{CBV}_{\text{static}}$  decreased from 18.5 [11.1–22.3]  $10^3 \mu\text{m}^3$  in healthy controls to 10.2 [7.1–17.1]  $10^3 \mu\text{m}^3$  in sepsis patients ( $p = 0.005$ ).

Next, we calculated capillary recruitment (CR) as 1- the slope( $V_{\text{RBC}} (D \leq 7 \mu\text{m})$ ,  $V_{\text{RBC}} (D \geq 10 \mu\text{m})$ ). CR per group decreased from 78% in healthy controls to 8% in sepsis patients (Fig. 3c). Finally, we calculated  $\text{CBV}_{\text{dynamic}}$  by multiplying  $\text{CBV}_{\text{static}}$  with  $(1 + \text{CR})$ .  $\text{CBV}_{\text{dynamic}}$  showed

a significant higher and much wider *normal* range in healthy controls compared to  $\text{CBV}_{\text{absolute}}$  and  $\text{CBV}_{\text{static}}$  respectively.  $\text{CBV}_{\text{dynamic}}$  decreased from 32.8 [19.7–39.5]  $10^3 \mu\text{m}^3$  in healthy controls to 11.1 [7.7–18.5]  $10^3 \mu\text{m}^3$  in sepsis patients ( $p < 0.0001$ ). Overall, we were able to show that by adding dynamic variables to CBV calculation, the discrimination between the groups could be significantly improved (Fig. 3d).

#### Derivation of an RBC velocity-adjusted perfused boundary region

We have previously shown that PBR values (averaged across all diameter classes from 5 to 25  $\mu\text{m}$ ) increase in sepsis patients [18–20], indicating sepsis-induced damage of the eGC. In this study,  $\text{PBR}_{\text{static}}$  ( $D$  4 to 25  $\mu\text{m}$ ) increased from 2.24 [2.13–2.35]  $\mu\text{m}$  in healthy controls to 2.48 [2.33–2.62]  $\mu\text{m}$  in sepsis patients ( $p < 0.0001$ ) (Fig. 4a). In sepsis patients,  $\text{PBR}_{\text{static}}$  showed a tendency to increase at low levels of feed vessel velocity, whereas in healthy controls,  $\text{PBR}_{\text{static}}$  showed a tendency to stay constant or even slightly decrease at low feed vessel velocity (Fig. 4b). To eliminate the influence of different RBC velocities on  $\text{PBR}_{\text{static}}$ , we estimated  $\text{PBR}_{\text{dynamic}}$  at a feed vessels  $V_{\text{RBC}}$  of 0  $\mu\text{m}/\text{s}$  based on the different slopes( $\text{PBR}_{\text{static}}$ ,  $V_{\text{RBC}} (D \geq 10 \mu\text{m})$ ) in healthy subjects and sepsis patients (Fig. 4b and Additional file 6: Fig. S4).  $\text{PBR}_{\text{dynamic}}$  increased from 1.95 [1.84–2.08]  $\mu\text{m}$  in healthy controls to 2.58 [2.43–2.76]  $\mu\text{m}$  in sepsis patients ( $p < 0.0001$ ) (Fig. 4c). In summary, adjustment of the PBR to  $V_{\text{RBC}}$  improved discrimination between the groups by about 50%.

#### Development of the Microvascular Health Score

We have previously shown, that glycocalyx damage and microcirculatory impairment do neither coincide, nor do they occur in proportion in every sepsis patient [20]. This un-coupling of changes in PBR and CBV can also be reproduced in the group of sepsis patients (Fig. 5a–c). To account for this finding, we combined the different variables into one Microvascular Health Score (MVHS<sup>TM</sup>) (Additional file 10: Fig. S7). Because CBV decreases and PBR increases in sepsis, we formed the quotient of  $\text{CBV} / \text{PBR}$  to calculate the MVHS in a static and a dynamic version ( $\text{MVHS}_{\text{static}} = \text{CBV}_{\text{static}} (D$  4 to 6  $\mu\text{m}) / \text{PBR}_{\text{static}} (D$  4 to 25  $\mu\text{m})$  and  $\text{MVHS}_{\text{dynamic}} = \text{CBV}_{\text{dynamic}} (D$  4 to 6  $\mu\text{m}) / \text{PBR}_{\text{dynamic}} (D$  4 to 25  $\mu\text{m})$ ).

The median  $\text{MVHS}_{\text{static}}$  was significantly lower in sepsis patients 1.70 [1.32–2.53] points compared to healthy controls 4.03 [2.11–4.33] points ( $p < 0.001$ ). The median  $\text{MVHS}_{\text{dynamic}}$  stressed the difference between sepsis patients and healthy controls (1.78 [1.38–2.67] vs. 7.43 [4.65–8.73] points,  $p < 0.0001$ ) even more than the  $\text{MVHS}_{\text{static}}$ .

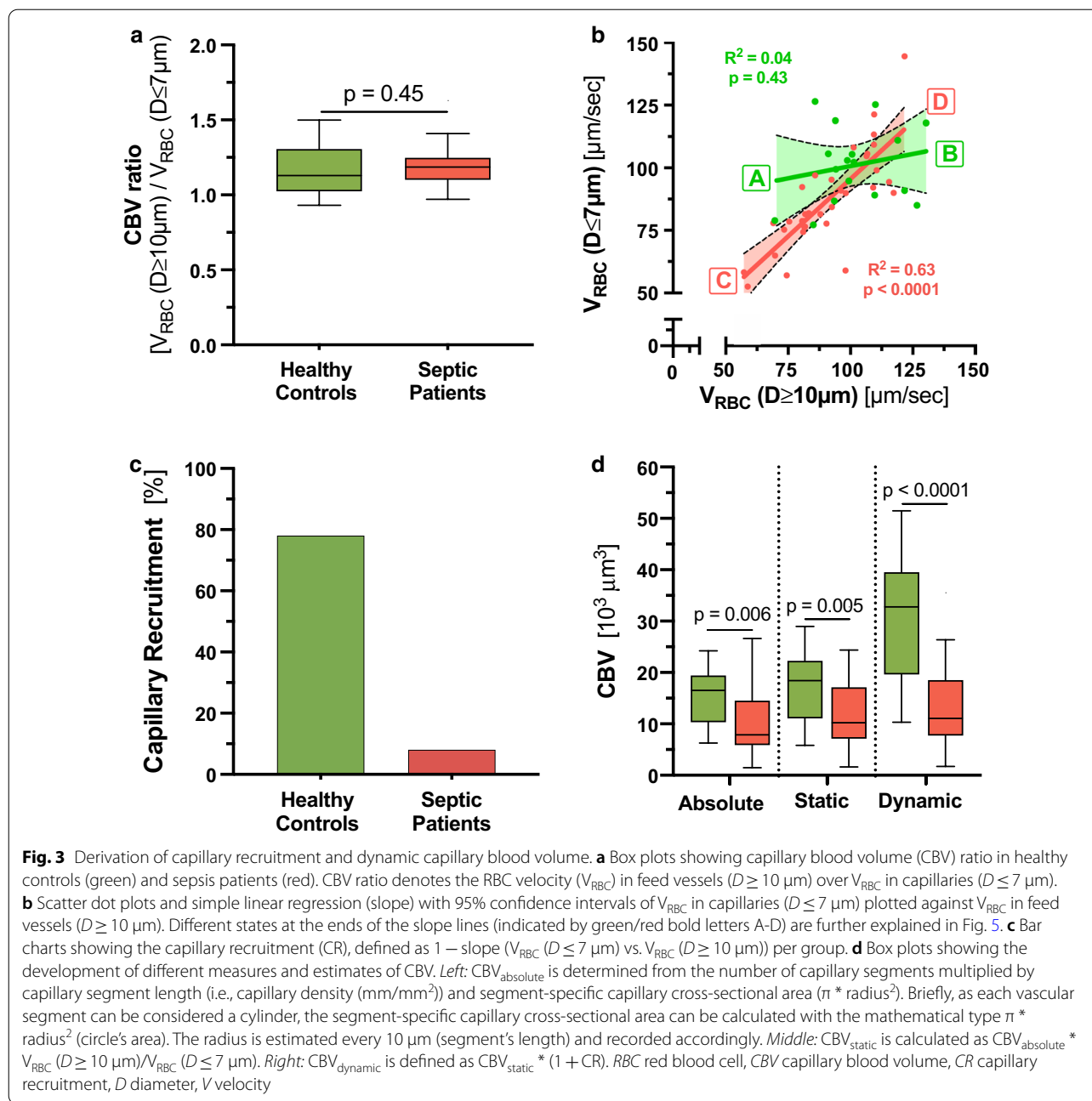


**Fig. 3** Derivation of capillary recruitment and dynamic capillary blood volume. **a** Box plots showing capillary blood volume (CBV) ratio in healthy controls (green) and sepsis patients (red). CBV ratio denotes the RBC velocity ( $V_{RBC}$ ) in feed vessels ( $D \geq 10 \mu m$ ) over  $V_{RBC}$  in capillaries ( $D \leq 7 \mu m$ ). **b** Scatter dot plots and simple linear regression (slope) with 95% confidence intervals of  $V_{RBC}$  in capillaries ( $D \leq 7 \mu m$ ) plotted against  $V_{RBC}$  in feed vessels ( $D \geq 10 \mu m$ ). Different states at the ends of the slope lines (indicated by green/red bold letters A-D) are further explained in Fig. 5. **c** Bar charts showing the capillary recruitment (CR), defined as  $1 - \text{slope} (V_{RBC} (D \leq 7 \mu m) \text{ vs. } V_{RBC} (D \geq 10 \mu m))$  per group. **d** Box plots showing the development of different measures and estimates of CBV. *Left:*  $CBV_{\text{absolute}}$  is determined from the number of capillary segments multiplied by capillary segment length (i.e., capillary density ( $\text{mm}/\text{mm}^2$ ) and segment-specific capillary cross-sectional area ( $\pi * \text{radius}^2$ )). Briefly, as each vascular segment can be considered a cylinder, the segment-specific capillary cross-sectional area can be calculated with the mathematical type  $\pi * \text{radius}^2$  (circle's area). The radius is estimated every  $10 \mu m$  (segment's length) and recorded accordingly. *Middle:*  $CBV_{\text{static}}$  is calculated as  $CBV_{\text{absolute}} * V_{RBC} (D \geq 10 \mu m) / V_{RBC} (D \leq 7 \mu m)$ . *Right:*  $CBV_{\text{dynamic}}$  is defined as  $CBV_{\text{static}} * (1 + CR)$ .  $RBC$  red blood cell,  $CBV$  capillary blood volume,  $CR$  capillary recruitment,  $D$  diameter,  $V$  velocity

**Association of the Microvascular Health Score (MVHS) with disease severity**

Both,  $MVHS_{\text{static}}$  and  $MVHS_{\text{dynamic}}$  correlated moderate-to-strong with SOFA score, number of dysfunctional organs, lactate, CRP, IL-6 and PCT (all  $p < 0.001$ ) in a pooled analysis that included healthy controls and sepsis patients (Table 2). These observations remained unchanged in additional sensitivity analyses (Additional file 7: Table A3).

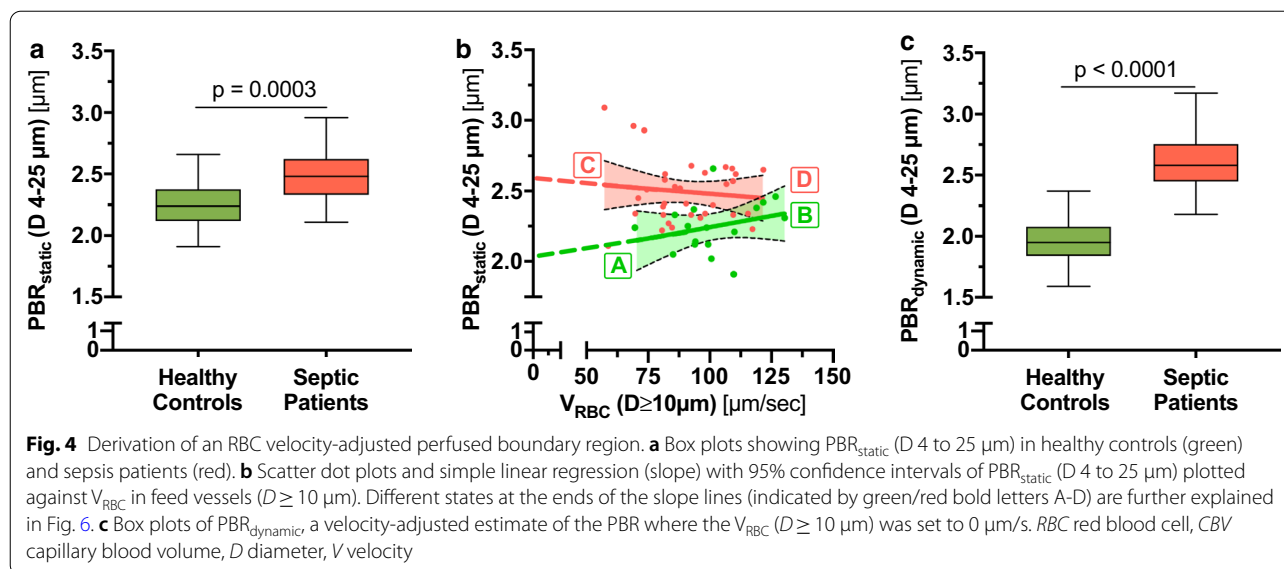
In the subgroup of sepsis patients, the correlations of  $MVHS_{\text{static}}$  and  $MVHS_{\text{dynamic}}$  with SOFA score and

number of dysfunctional organs remained significant (all  $p \leq 0.01$ ) (Table 2 and Additional file 7: Table A4).  $MVHS_{\text{dynamic}}$  was significantly different in sepsis subgroups stratified by either median SOFA score or median number of dysfunctional organs, respectively (Fig. 5d and Additional file 11: Fig. S8).

**Discussion**

In this study, we employed a differentiated, diameter class-wise analysis of RBC kinetics to identify novel variables of microvascular dysfunction in sepsis. This





approach revealed several size- and group-specific characteristics of the measured variables within the diameter-range from 4 to 25  $\mu m$ . Accordingly, we propose the  $MVHS_{dynamic}$ , which has a broad bandwidth to detect microvascular (dys-)function in healthy subjects and critically ill patients. To our knowledge, the  $< 20 \mu m$  range has neither been divided into single  $\mu m$ -steps nor individually examined and compared with clinical information from healthy and septic subjects before.

### Capillary recruitment

Observing that RBC dynamics differ between capillaries ( $D \leq 7 \mu m$ ) and feeding vessels ( $D \geq 10 \mu m$ ) led us to relate capillaries and feeding vessels to each other—which resulted in the calculation of capillary recruitment. The concept of capillary recruitment in skeletal muscle was first proposed by August Krogh in 1919 [29]. Krogh hypothesized that the opening of previously closed muscle capillaries, i.e., capillary recruitment, would allow capillary RBC velocities to remain low, and capillary oxygen extraction thereby efficient, despite large increases in blood supply. While the binary distinction between "closed" and "open" capillaries, was key to Krogh's model argument, modern observations suggest that capillary recruitment should be regarded rather in the context of continuous than binary changes in RBC distributions and velocities among capillaries [30, 31]. In this respect, our quantitative data show that healthy individuals (at least under resting conditions) have relatively constant median capillary RBC velocities, which seems to be independent of the associated  $V_{RBC}$  in the feed vessels. Even though the underlying (auto-) regulation mechanisms remain incompletely understood, compliance with a narrow RBC

velocity range seems plausible to guarantee an optimal supply–demand ratio in capillaries. Conceptually, *constant* capillary RBC velocities in the face of varying  $V_{RBC}$  in larger feeding vessels is consistent with a) increasing numbers of RBC-perfused capillaries at tissue sites with higher metabolic demand and increased blood supply in feeding vessels, as well as b) reduced numbers of RBC-perfused capillaries at sites with lower metabolic demand and reduced feeding vessel blood supply. The failure to maintain constant RBC velocities in capillaries of patients with sepsis and the fact that capillary RBC velocities in our septic cohort change proportionally with RBC velocity changes in feedings vessels, reflects that the number of perfused capillaries in sepsis patients is *fixed* and insensitive to local variations in tissue metabolic demand. A simplified version of the pathophysiologic concept of capillary (de-)recruitment observed in this study is visualized in Fig. 6.

Estimates of capillary recruitment in our cohort are based on *per group* analysis of relations between RBC velocities in capillaries and feeding vessels. New recording and analysis strategies that allow for calculation of capillary recruitment on a per-patient basis are currently under investigation. This modification will allow for capturing enough low- and high flow situations per subject to generate intra-individual regression slopes. Thus, it will be possible to determine the capillary recruitment *per individual subject*, which might further improve discrimination of dynamic variables, such as  $CBV_{dynamic}$  and  $MVHS_{dynamic}$ .

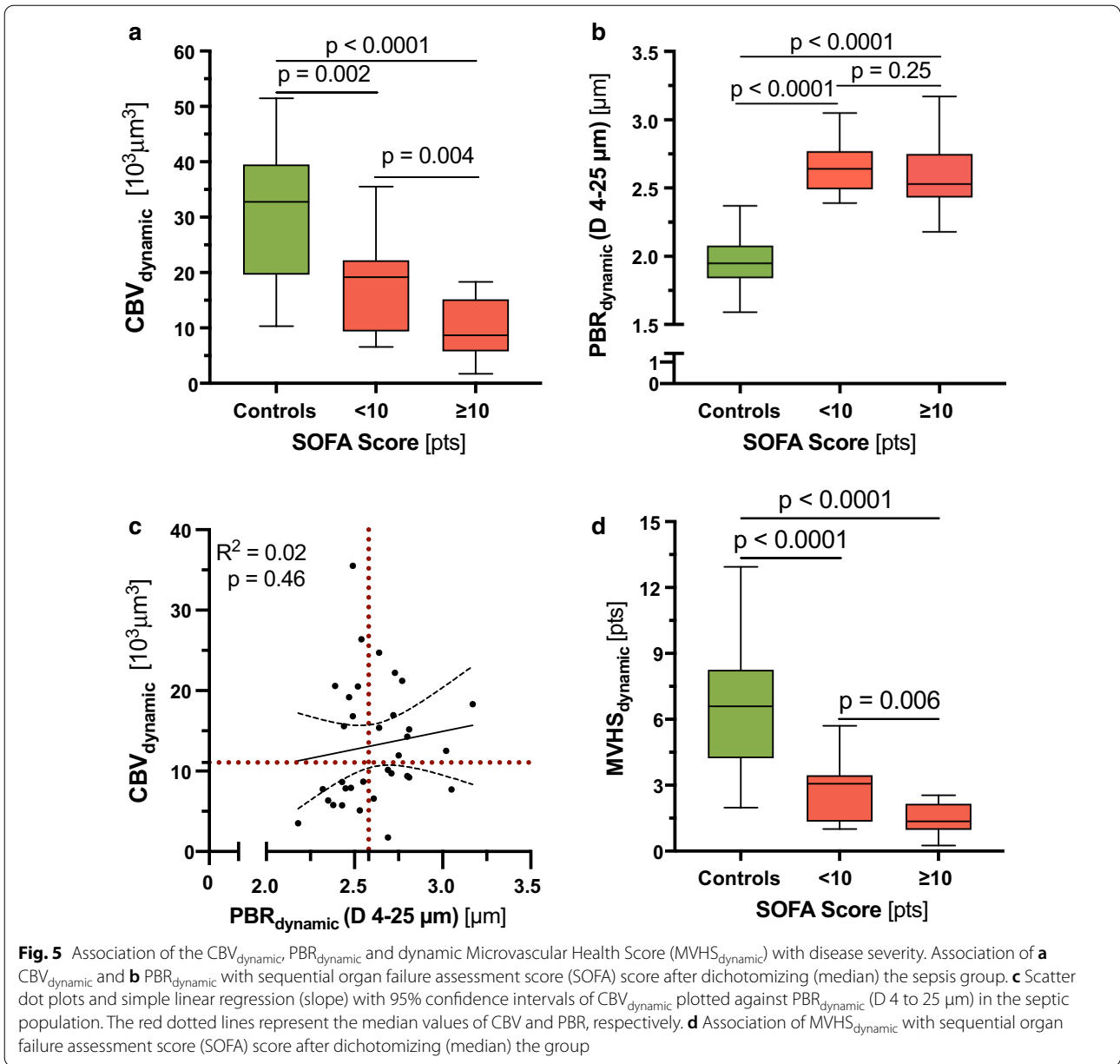


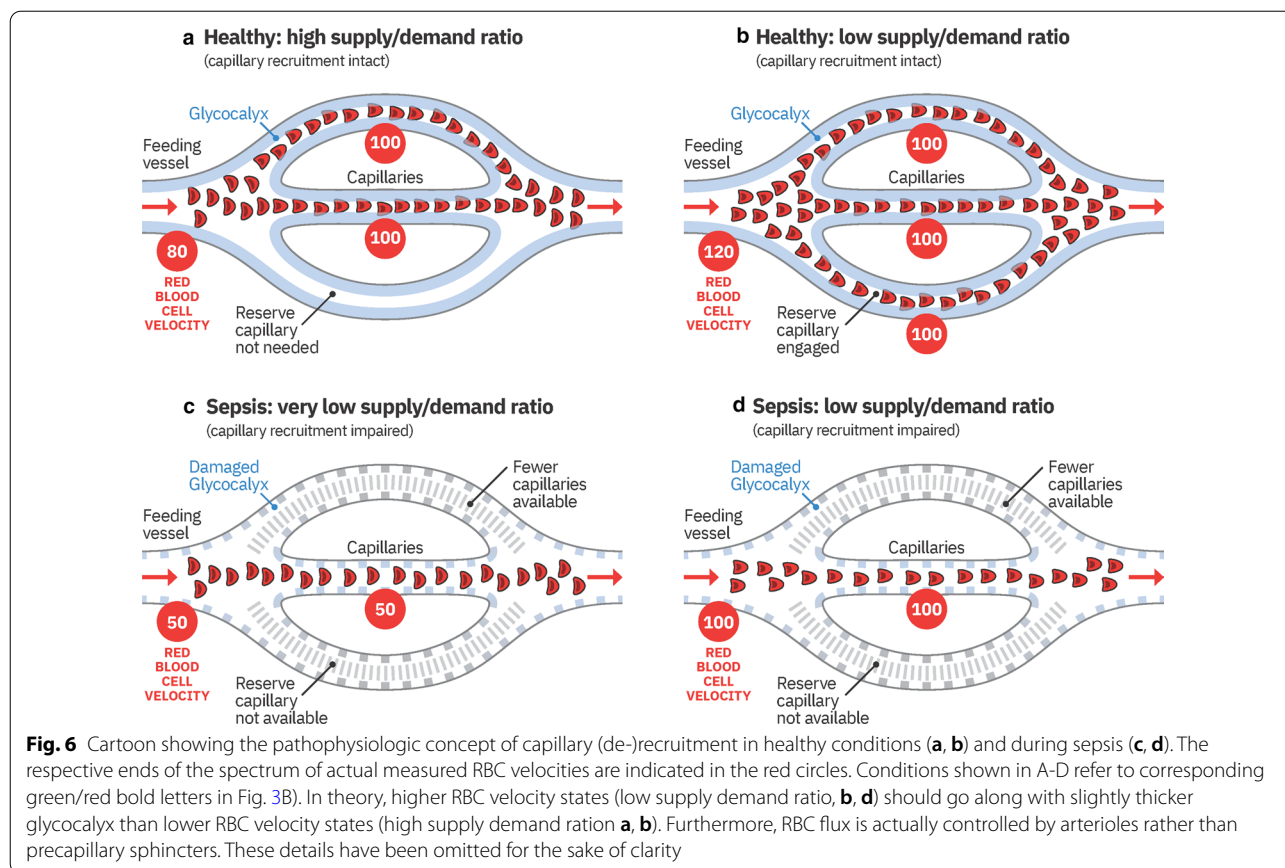
**Fig. 5** Association of the  $CBV_{dynamic}$ ,  $PBR_{dynamic}$  and dynamic Microvascular Health Score ( $MVHS_{dynamic}$ ) with disease severity. Association of **a**  $CBV_{dynamic}$  and **b**  $PBR_{dynamic}$  with sequential organ failure assessment score (SOFA) score after dichotomizing (median) the sepsis group. **c** Scatter dot plots and simple linear regression (slope) with 95% confidence intervals of  $CBV_{dynamic}$  plotted against  $PBR_{dynamic}$  (D 4 to 25  $\mu m$ ) in the septic population. The red dotted lines represent the median values of  $CBV$  and  $PBR$ , respectively. **d** Association of  $MVHS_{dynamic}$  with sequential organ failure assessment score (SOFA) score after dichotomizing (median) the group

**Table 2** Correlations of  $MVHS$  with clinical variables

Variable	Controls & sepsis patients (n = 51)		Sepsis patients (n = 34)	
	$MVHS_{static}$	$MVHS_{dynamic}$	$MVHS_{static}$	$MVHS_{dynamic}$
SOFA Score (points)	-0.57 ( $p < 0.0001$ )	-0.77 ( $p < 0.0001$ )	-0.43 ( $p = 0.01$ )	-0.44 ( $p = 0.01$ )
Number of dysfunctional organs (n)	-0.60 ( $p < 0.0001$ )	-0.80 ( $p < 0.0001$ )	-0.51 ( $p = 0.002$ )	-0.52 ( $p = 0.002$ )
Lactate (mmol/l)	-0.37 ( $p = 0.007$ )	-0.42 ( $p = 0.002$ )	-0.23 ( $p = 0.19$ )	-0.22 ( $p = 0.20$ )
CRP (mg/dl)	-0.39 ( $p = 0.005$ )	-0.61 ( $p < 0.0001$ )	0.02 ( $p = 0.92$ )	0.02 ( $p = 0.92$ )
IL6 (ng/ml)	-0.48 ( $p = 0.001$ )	-0.69 ( $p < 0.0001$ )	-0.14 ( $p = 0.48$ )	-0.14 ( $p = 0.48$ )
PCT (ng/ml)	-0.47 ( $p < 0.0001$ )	-0.68 ( $p < 0.0001$ )	-0.27 ( $p = 0.13$ )	-0.27 ( $p = 0.13$ )

Spearman correlation was used. The  $p$  values are indicated in brackets

CRP C-reactive protein, IL-6 interleukin-6,  $MVHS$  microvascular health score, PCT procalcitonin, SOFA Score sequential organ failure assessment score



### Endothelial glycocalyx damage

The sepsis-associated PBR increase measured in this study is consistent with changes observed in previous studies [18–20, 32–34]. The current study shows that adjustment of PBR estimates to  $V_{RBC}$  improved discrimination between the groups by about 50%. This gain in discriminatory power is important, as PBR estimates have so far shown a considerable overlap between healthy controls and sepsis patients. This adjustment accounts for RBC velocity dependency of the glycocalyx [35, 36]. Especially in sepsis patients, PBR tends to increase when RBC velocity decreases, suggesting that glycocalyx extends towards a more porous and permeable compartment in the absence of exposure to fluid/RBC shear forces. The fact that PBR increases are more extreme in the sepsis patients, is consistent with previous studies showing that glycocalyx is damaged and more permeable in sepsis, which likely contributes to its increased RBC velocity dependency. However, it is difficult to estimate if the higher PBR observed in sepsis patients is caused solely by real glycocalyx damage (i.e., enzymatic shedding [18, 37]) or if temporary and functional changes that enable nutrient and solute supply to

the interstitial space contribute to that PBR increase. We have previously shown that PBR estimates correlate excellent with glycocalyx thickness measured by atomic-force microscopy in cultured endothelial cells exposed to concordant sera from healthy subjects and sepsis patients [18, 20]. Glycocalyx damage in vitro was completely abolished when enzymatic activity of heparanase, a heparan sulphate specific endo-beta-D-glucuronidase, was blocked by addition of heparin [18]. Furthermore, circulating levels of Syndecan-1, a core protein of the intact glycocalyx, increased tenfold in sepsis patients and correlated with PBR values [20], indicating that enzymatic shedding is a dominant mechanism of PBR increase in sepsis. Elegant work in the cremasteric microcirculation showed that, inflammation-induced glycocalyx shedding increases effective capillary diameter. This effect is, however, defeated by enhanced white blood cell (WBC)-endothelial interactions and subsequent venular WBC obstruction, resulting in a net reduction of capillary  $V_{RBC}$  [38]. Glycocalyx damage may therefore partly explain the trend towards lower  $V_{RBC}$  in capillaries.

### Microvascular health score

In the current cross-sectional cohort, the proposed  $MVHS_{static}$  and  $MVHS_{dynamic}$  did correlate with SOFA score and number of dysfunctional organs in the subgroup of sepsis patients. Correlations between classical variables of the microcirculation and the SOFA score have been rarely reported. The SOFA correlated negatively with microvascular flow indices (MFI) as well as total and perfused vascular densities (TVD and PVD) in sepsis patients receiving activated protein C [33]. However, we couldn't detect any significant correlations of MFI, TVD or PVD with the SOFA score in a previous sepsis study [20]. The finding that the MVHS performed better than its individual components is a strong argument for combining different measures of microvascular dysfunction such as vascular blood volume (CBV) and glycocalyx properties (PBR) into one score. In our view, in particular the combination of CBV and PBR makes sense, because CBV and PBR appear to behave independently of each other [20], and may thus indicate different aspects of microvascular dysfunction. To clarify whether the MVHS can indeed predict relevant outcome in sepsis patients, we initiated two prospective, observational, longitudinal studies to evaluate the MVHS in the emergency room (Early Detection of Glycocalyx Damage in Emergency Room Patients—the EDGE Study, Clinicaltrials.gov Identifier: NCT03126032) and in the ICU (Analysis of Sublingual Glycocalyx Damage at ICU Admission to Predict Risk of Death—the ASGARD Study, Clinicaltrials.gov Identifier: NCT03847493). In these studies, serial measurements can possibly reveal differential changes in individual components of the MVHS in response to the initial therapy.

### Limitations

We acknowledge some limitations of our study. First, it is a single-center study with a limited sample size. Therefore, the findings cannot be directly generalized for all sepsis patients. However, the interdependencies between our novel variables and their associations with clinical variables remained significant after multiple adjustments and additional sensitivity analyses. Second, this study was neither designed nor powered to test the performance of novel variables for outcome prediction. However, our findings add interesting new aspects to the lively field of intravital microscopy research. Further longitudinal studies are needed to evaluate the MVHS for outcome prediction. Third, since all calculations are ultimately based on the flow properties of RBCs, we can only analyze microvessels in which a minimal number of RBCs are present and the predefined quality criteria are met. Vessels without RBCs or invalid vascular segments are

therefore not detected by the software. That could have an impact not only on the density calculations, but also on the estimation of the PBR, as severely affected capillaries might not be accessible to RBCs anymore. However, past studies have shown, that the average PBR (4–25  $\mu\text{m}$ ) of healthy and septic subjects measured in vivo correlates excellently with the decrease in glycocalyx thickness of endothelial cells after incubation with the concordant serum samples, further supporting the accuracy of PBR values. Fourth, technical limitations, as, e.g., pressure artifacts or low spatial resolution might have affected the results. However, all measurements were performed by only one very experienced investigator specially trained to avoid pressure artifacts. Moreover, the camera has a sufficiently high resolution.

### Conclusion and outlook

We used a highly differentiated analysis to quantify RBC dynamics in sublingual microvessels and found that taking the interdependence between capillary blood volume, capillary recruitment and PBR into account, is key to better understand microvascular dysfunction in sepsis. The  $MVHS_{dynamic}$  reflects an impairment of very small capillaries and has a broad bandwidth to detect microvascular dysfunction in critically ill patients. Future clinical studies should evaluate the prognostic value of MVHS in sepsis.

### Abbreviations

ASGARD: Analysis of Sublingual Glycocalyx Damage at ICU Admission to Predict Risk of Death; BMI: Body mass index; CBV: Capillary blood volume; CCI score: Charlson Comorbidity Index; CR: Capillary recruitment; CRP: C-reactive protein; D: Diameter; EDGE: Early detection of glycocalyx damage in emergency room patients; FDR: False discovery rate; Hb: Hemoglobin; ICU: Intensive care unit; IL-6: Interleukin-6; IQR: Interquartile range; MAP: Mean arterial pressure; MFI: Microvascular flow index; MVHS: Microvascular health score; PBR: Perfused boundary region; PCT: Procalcitonin; PVD: Perfused vascular density; RBC: Red blood cell; RBCW: Red blood cell width; SDF: Sidestream dark field; SOFA score: Sequential Organ Failure Assessment score; TVD: Total vascular density; UKM: University Hospital Münster;  $V_{RBC}$ : Red blood cell velocity; WBC: White blood cell.

### Supplementary Information

The online version contains supplementary material available at <https://doi.org/10.1186/s13054-021-03520-w>.

**Additional file 1: Fig. S1.** Screenshots of randomly selected videos of one healthy (A–B) and four sepsis (C–J) individuals. Left: Screenshots without showing automatic vessel detection. Right: Vessels with diameter between 4 and 25  $\mu\text{m}$  of the images on the left column are automatically highlighted and subjected to an automatic quality check. Invalid vascular segments are marked yellow and are automatically discarded, while all valid vascular segments (green lines) are further analyzed (see Figure 1).

**Additional file 2: Video 1.** Measurement of a healthy individual with and without automatic vessel detection and segments' analysis.

**Additional file 3: Video 2.** Measurement of a sepsis patient with and without automatic vessel detection and segments' analysis.

**Additional file 4: Fig. S2.** Correlation between manually and automatically measurement of  $V_{RBC}$ . Average manually derived longitudinal RBC movement per vessel was plotted against automatically measured  $V_{RBC}$  of the same specific vessel (Spearman correlation). For manual validation of  $V_{RBC}$ , 15 vessels (diameter 5 to 17  $\mu\text{m}$ ) from 3 randomly selected movies were analyzed manually. Therefore, longitudinal movement of individual RBCs in that vessels were tracked and measured as pixels per frame through subsequent vascular segments. Measured pixels per frame were transformed to  $\mu\text{m}/\text{sec}$  using camera frame-rate and pixel size.

**Additional file 5: Fig. S3.** Derivation of capillary recruitment. The capillary recruitment is calculated by the slope of the relationship between  $V_{RBC}$  ( $D \leq 7 \mu\text{m}$ ) and  $V_{RBC}$  ( $D \geq 10 \mu\text{m}$ ). Two examples: In case capillary blood volume doubles when large vessel RBC velocity increases 2-fold, the slope ( $V_{RBC}$  ( $D \leq 7 \mu\text{m}$ ),  $V_{RBC}$  ( $D \geq 10 \mu\text{m}$ )) will be 0 and  $CR = 1 - \text{slope } 0 = 1 = 100\%$ . In the absence of changes in capillary blood volume when  $V_{RBC}$  ( $D \geq 10 \mu\text{m}$ ) increases 2-fold, capillary RBC velocities are expected to also change proportionally by 2-fold, and the slope of  $V_{RBC}$  ( $D \leq 7 \mu\text{m}$ ) vs.  $V_{RBC}$  ( $D \geq 10 \mu\text{m}$ ) will be 1 and  $CR = 1 - \text{slope } 1 = 0 = 0\%$ .

**Additional file 6: Fig. S4.** Derivation of  $PBR_{dynamic}$  from  $PBR_{static}$ . All dots are shifted to  $V = 0 \mu\text{m}/\text{sec}$  parallelly to the slopes of each group.

**Additional file 7: Table A1.** Comorbidities, focus of infection and isolated pathogens in the septic cohort. **Table A2.** Correlation coefficient between microvascular and clinical variables shown in Figure 1B, D, F. **Table A3.** Sensitivity analysis in sepsis patients and healthy controls. **Table A4.** Sensitivity analysis in sepsis patients.

**Additional file 8: Fig. S5.** Capillary dropout in sepsis patients. Bar charts showing the percentage of loss of vascular density in sepsis patients compared to healthy controls. Q value (adjusted P value): \* $q < 0.05$ , \*\* $q < 0.01$ , \*\*\* $q < 0.001$

**Additional file 9: Fig. S6.** Pooled  $PBR_{static}$  values in predefined diameter ranges. Boxplots of  $PBR_{static}$  values of healthy controls and septic patients based on the different microvascular diameter ranges as output by the previous version of the GlycoCheck™ software used in [20].

**Additional file 10: Fig. S7.** Conceptual development of the dynamic version of Microvascular Health score ( $MVHS_{dynamic}$ )

**Additional file 11: Fig. S8.** Association of  $MVHS_{dynamic}$  with numbers of dysfunctional organs in sepsis patients (red) after dichotomizing (median) the group.

#### Acknowledgements

We would like to acknowledge the support of the Open Access Publication Fund of the University of Münster.

#### Authors' contributions

AR designed the study, performed the measurements, recorded clinical data, analyzed the data, prepared the figures, and contributed to the manuscript; JS recruited patients and reviewed the manuscript; SK retrieved clinical and microbiologic data and reviewed the manuscript; HP and JR contributed to the design of the study, discussed the findings and reviewed the manuscript; HV developed and refined the Glycocheck™ methodology, invented the novel variables, analyzed the data and contributed to the manuscript; PK had the initial idea, supervised the study, prepared the figures and drafted the manuscript. All authors read and approved the final manuscript.

#### Funding

Open Access funding enabled and organized by Projekt DEAL. This work was supported by the German Research Foundation (KFO342) to AR, PK (KU 2873/3-1) and JR (RO 4537/5-1). The funding body had no role in the design of the study, collection, analysis and interpretation of data or in writing the manuscript.

#### Availability of data and materials

The datasets used and/or analyses during the current study are available from the corresponding author on reasonable request.

## Declarations

#### Ethics approval and consent to participate

The study was performed in accordance with the Declaration of Helsinki and approved by the Ethics Committee of the General Medical Council Westfalen-Lippe and the WWU Münster, Germany (file number: amendment to 2016–073-f-5). Informed consent was obtained.

#### Consent for publication

Consent for publication has been obtained. Written informed consent has been obtained from all identifiable individuals.

#### Competing interests

AR, JS, JR, SK, HP, and PK declare that they have no competing interests. HV is Chief Science Officer of GlycoCheck™ BV, The Netherlands. GlycoCheck™ and MVHS™ are trademarks registered by Microvascular Health Solutions LLC (Alpine, UT, United States).

#### Author details

<sup>1</sup> Department of Medicine D, Division of General Internal and Emergency Medicine, Nephrology, and Rheumatology, University Hospital Münster, Albert-Schweitzer-Campus 1, 48149 Münster, Germany. <sup>2</sup> Department of Cardiology and Angiology, University Hospital Münster, Albert-Schweitzer-Campus 1, 48149 Münster, Germany. <sup>3</sup> Department of Anesthesiology, Intensive Care and Pain Medicine, University Hospital Münster, Albert-Schweitzer-Campus 1, 48149 Münster, Germany. <sup>4</sup> Institute of Hygiene, University Hospital Münster, Albert-Schweitzer-Campus 1, 48149 Münster, Germany. <sup>5</sup> Department of Physiology, Cardiovascular Research Institute Maastricht, Maastricht University, Maastricht, The Netherlands.

Received: 12 October 2020 Accepted: 1 March 2021

Published online: 19 March 2021

#### References

- Ince C, De Backer D, Mayeux PR. Microvascular Dysfunction in the Critically Ill. Crit Care Clin. 2020;36(2):323–31. <https://doi.org/10.1016/j.ccc.2019.11.003>.
- Pool R, Gomez H, Kellum JA. Mechanisms of Organ Dysfunction in Sepsis. Crit Care Clin. 2018;34(1):63–80. <https://doi.org/10.1016/j.ccc.2017.08.003>.
- Rossaint J, Zarbock A. Pathogenesis of Multiple Organ Failure in Sepsis. Crit Rev Immunol. 2015;35(4):277–91. <https://doi.org/10.1615/critrevimmunol.2015015461>.
- Bezemer R, Bartels SA, Bakker J, Ince C. Clinical review: Clinical imaging of the sublingual microcirculation in the critically ill—where do we stand? Crit Care. 2012;16(3):224. <https://doi.org/10.1186/cc11236>.
- De Backer D. Is microcirculatory assessment ready for regular use in clinical practice? Curr Opin Crit Care. 2019;25(3):280–4. <https://doi.org/10.1097/MCC.0000000000000605>.
- Ince C, Boerma EC, Cecconi M, De Backer D, Shapiro NI, Duranteau J, Pinsky MR, Artigas A, Teboul JL, Reiss IKM, et al. Second consensus on the assessment of sublingual microcirculation in critically ill patients: results from a task force of the European Society of Intensive Care Medicine. Intensive Care Med. 2018;44(3):281–99. <https://doi.org/10.1007/s00134-018-5070-7>.
- Pranskunas A, Koopmans M, Koetsier PM, Pilvinis V, Boerma EC. Microcirculatory blood flow as a tool to select ICU patients eligible for fluid therapy. Intensive Care Med. 2013;39(4):612–9. <https://doi.org/10.1007/s00134-012-2793-8>.
- Massey MJ, Hou PC, Filbin M, Wang H, Ngo L, Huang DT, Aird WC, Novack V, Trzeciak S, Yealy DM, et al. Microcirculatory perfusion disturbances in septic shock: results from the ProCESS trial. Crit Care. 2018;22(1):308. <https://doi.org/10.1186/s13054-018-2240-5>.
- Hutchings SD, Naumann DN, Hopkins P, Mellis C, Riozzi P, Sartini S, Mamuzaj J, Harris T, Midwinter MJ, Wendon J. Microcirculatory impairment is associated with multiple organ dysfunction following traumatic hemorrhagic shock: the MICROSHOCK study. Crit Care Med. 2018;46(9):e889–96. <https://doi.org/10.1097/CCM.0000000000003275>.



10. Scorcella C, Damiani E, Domizi R, Pierantozzi S, Tondi S, Carsetti A, Ciucani S, Monaldi V, Rogani M, Marini B, et al. MicroDAIMON study: Microcirculatory Dally monitoring in critically ill patients: a prospective observational study. *Ann Intensive Care*. 2018;8(1):64. <https://doi.org/10.1186/s13613-018-0411-9>.
11. Vellinga NA, Boerma EC, Koopmans M, Donati A, Dubin A, Shapiro NI, Pearse RM, Machado FR, Fries M, Akarsu-Ayazoglu T, et al. International study on microcirculatory shock occurrence in acutely ill patients. *Crit Care Med*. 2015;43(1):48–56. <https://doi.org/10.1097/CCM.0000000000000553>.
12. Vellinga NAR, Boerma EC, Koopmans M, Donati A, Dubin A, Shapiro NI, Pearse RM, van der Voort PHJ, Dondorp AM, Bafi T, et al. Mildly elevated lactate levels are associated with microcirculatory flow abnormalities and increased mortality: a microSOAP post hoc analysis. *Crit Care*. 2017;21(1):255. <https://doi.org/10.1186/s13054-017-1842-7>.
13. De Backer D, Donadello K, Sakr Y, Ospina-Tascon G, Salgado D, Scolletta S, Vincent JL. Microcirculatory alterations in patients with severe sepsis: impact of time of assessment and relationship with outcome. *Crit Care Med*. 2013;41(3):791–9. <https://doi.org/10.1097/CCM.0b013e3182742e8b>.
14. Watchorn JC, Fargaly H, Gilani M, Assadi J, Deitchman AR, Naumann DN, Wollborn J, Goebel U, McCurdy MT, Hutchings SD. The reproducibility of the point of care microcirculation (poem) score when used to assess critically ill patients: a multicenter prospective observational study. *Shock*. 2019. <https://doi.org/10.1097/SHK.0000000000001474>.
15. Sardinha J, MacKinnon S, Lehmann C. Rapid clinical assessment of the sublingual microcirculation—visual scoring using microVAS in comparison to standard semi-automated analysis. *Clin Hemorheol Microcirc*. 2019;72(3):229–38. <https://doi.org/10.3233/CH-180427>.
16. Carsetti A, Aya HD, Pierantozzi S, Bazurro S, Donati A, Rhodes A, Cecconi M. Ability and efficiency of an automatic analysis software to measure microvascular parameters. *J Clin Monit Comput*. 2017;31(4):669–76. <https://doi.org/10.1007/s10077-016-9928-3>.
17. Hilty MP, Guerci P, Ince Y, Toraman F, Ince C. MicroTools enables automated quantification of capillary density and red blood cell velocity in handheld vital microscopy. *Commun Biol*. 2019;2:217. <https://doi.org/10.1038/s42003-019-0473-8>.
18. Drost CC, Rovas A, Kusche-Vihrog K, Van Slyke P, Kim H, Hoang VC, Maynes JT, Wennmann DO, Pavenstadt H, Linke W, et al. Tie2 activation promotes protection and reconstitution of the endothelial glycocalyx in human sepsis. *Thromb Haemost*. 2019;119(11):1827–38. <https://doi.org/10.1055/s-0039-1695768>.
19. Rovas A, Lukasz AH, Vink H, Urban M, Sackarnd J, Pavenstadt H, Kumpers P. Bedside analysis of the sublingual microvascular glycocalyx in the emergency room and intensive care unit - the GlycoNurse study. *Scand J Trauma Resusc Emerg Med*. 2018;26(1):16. <https://doi.org/10.1186/s13049-018-0483-4>.
20. Rovas A, Seidel LM, Vink H, Pohlkötter T, Pavenstadt H, Ertmer C, Hessler M, Kumpers P. Association of sublingual microcirculation parameters and endothelial glycocalyx dimensions in resuscitated sepsis. *Crit Care*. 2019;23(1):260. <https://doi.org/10.1186/s13054-019-2542-2>.
21. Hesse B, Rovas A, Buscher K, Kusche-Vihrog K, Brand M, Di Marco GS, Kielstein JT, Pavenstadt H, Linke WA, Nofer JR, et al. Symmetric dimethylarginine in dysfunctional high-density lipoprotein mediates endothelial glycocalyx breakdown in chronic kidney disease. *Kidney Int*. 2020;97(3):502–15. <https://doi.org/10.1016/j.kint.2019.10.017>.
22. Singer M, Deutschman CS, Seymour CW, Shankar-Hari M, Annane D, Bauer M, Bellomo R, Bernard GR, Chiche JD, Coopersmith CM, et al. The third international consensus definitions for sepsis and septic shock (Sepsis-3). *JAMA*. 2016;315(8):801–10. <https://doi.org/10.1001/jama.2016.0287>.
23. Quan H, Li B, Couris CM, Fushimi K, Graham P, Hider P, Januel JM, Sundararajan V. Updating and validating the Charlson comorbidity index and score for risk adjustment in hospital discharge abstracts using data from 6 countries. *Am J Epidemiol*. 2011;173(6):676–82. <https://doi.org/10.1093/aje/kwq433>.
24. Dane MJ, Khairoun M, Lee DH, van den Berg BM, Eskens BJ, Boels MG, van Teeffelen JW, Rops AL, van der Vlag J, van Zonneveld AJ, et al. Association of kidney function with changes in the endothelial surface layer. *Clin J Am Soc Nephrol*. 2014;9(4):698–704. <https://doi.org/10.2215/CJN.08160813>.
25. Lee DH, Dane MJ, van den Berg BM, Boels MG, van Teeffelen JW, de Mutsert R, den Heijer M, Rosendaal FR, van der Vlag J, van Zonneveld AJ, et al. Deeper penetration of erythrocytes into the endothelial glycocalyx is associated with impaired microvascular perfusion. *PLoS ONE*. 2014;9(5):e96477. <https://doi.org/10.1371/journal.pone.0096477>.
26. Diez-Silva M, Dao M, Han J, Lim CT, Suresh S. Shape and biomechanical characteristics of human red blood cells in health and disease. *MRS Bull*. 2010;35(5):382–8. <https://doi.org/10.1557/mrs2010.571>.
27. Hulley SB CS, Browner WS, Grady D, Newman TB. Designing clinical research : an epidemiologic approach. In., 4th edn. Philadelphia, PA: Lippincott Williams & Wilkins; 2013: Appendix 6C, p. 79.
28. Zhang CE, Staals J, van Oostenbrugge RJ, Vink H. Uncoupling of microvascular blood flow and capillary density in vascular cognitive impairment. *Front Neurol*. 2019;10:1268. <https://doi.org/10.3389/fneur.2019.01268>.
29. Krogh A. The supply of oxygen to the tissues and the regulation of the capillary circulation. *J Physiol*. 1919;52(6):457–74. <https://doi.org/10.1113/jphysiol.1919.sp001844>.
30. Angley's H, Ostergaard L. Krogh's capillary recruitment hypothesis, 100 years on: Is the opening of previously closed capillaries necessary to ensure muscle oxygenation during exercise? *Am J Physiol Heart Circ Physiol*. 2020;318(2):H425–47. <https://doi.org/10.1152/ajpheart.00384.2019>.
31. Poole DC, Copp SW, Ferguson SK, Musch TI. Skeletal muscle capillary function: contemporary observations and novel hypotheses. *Exp Physiol*. 2013;98(12):1645–58. <https://doi.org/10.1113/expphysiol.2013.073874>.
32. Donati A, Damiani E, Domizi R, Romano R, Adrario E, Pelaia P, Ince C, Singer M. Alteration of the sublingual microvascular glycocalyx in critically ill patients. *Microvasc Res*. 2013;90:86–9. <https://doi.org/10.1016/j.mvr.2013.08.007>.
33. Donati A, Damiani E, Botticelli L, Adrario E, Lombardo MR, Domizi R, Marini B, Van Teeffelen JW, Carletti P, Girardis M, et al. The aPC treatment improves microcirculation in severe sepsis/septic shock syndrome. *BMC Anesthesiol*. 2013;13(1):25. <https://doi.org/10.1186/1471-2253-13-25>.
34. Pranskunas A, Tamosuitis T, Balciuniene N, Damanskyte D, Sneider E, Vitkauskienė A, Sirvinskis E, Pilvinis V, Boerma EC. Alterations of conjunctival glycocalyx and microcirculation in non-septic critically ill patients. *Microvasc Res*. 2018;118:44–8. <https://doi.org/10.1016/j.mvr.2018.02.004>.
35. Wang G, Kostidis S, Tiemeier GL, Sol W, de Vries MR, Giera M, Carmeliet P, van den Berg BM, Rabelink TJ. Shear stress regulation of endothelial glycocalyx structure is determined by glucobiosynthesis. *Arterioscler Thromb Vasc Biol*. 2020;40(2):350–64. <https://doi.org/10.1161/ATVBAHA.119.313399>.
36. Harding IC, Mitra R, Mensah SA, Nersesyan A, Bal NN, Ebong EE. Endothelial barrier reinforcement relies on flow-regulated glycocalyx, a potential therapeutic target. *Biorheology*. 2019;56(2–3):131–49. <https://doi.org/10.3233/BIOR-180205>.
37. Wiesinger A, Peters W, Chappell D, Kentrup D, Reuter S, Pavenstadt H, Oberleithner H, Kumpers P. Nanomechanics of the endothelial glycocalyx in experimental sepsis. *PLoS ONE*. 2013;8(11):e80905. <https://doi.org/10.1371/journal.pone.0080905>.
38. Lipowsky HH, Gao L, Lescanic A. Shedding of the endothelial glycocalyx in arterioles, capillaries, and venules and its effect on capillary hemodynamics during inflammation. *Am J Physiol Heart Circ Physiol*. 2011;301(6):H2235–2245. <https://doi.org/10.1152/ajpheart.00803.2011>.

## Publisher's Note

Springer Nature remains neutral with regard to jurisdictional claims in published maps and institutional affiliations.